Coexistence of {011} facets with {112} facets on W(111) induced by ultrathin films of Pd

C.-H. Nien and T. E. Madey*
Department of Physics and Astronomy, and Laboratory for Surface Modification, Rutgers, The State University of New Jersey, Piscataway, New Jersey 08854

Y. W. Tai and T. C. Leung
Department of Physics, National Chung Cheng University, Chia-Yi 621, Taiwan

J. G. Che† and C. T. Chan*
Physics Department, Hong Kong University of Science and Technology, Clear Water Bay, Hong Kong, China
(Received 15 July 1998)

The faceting of Pd/W(111) to form nanoscale three-sided pyramids with {011} facets has been observed using a scanning tunneling microscope (STM). In contrast to the well-documented {112} faceting, which can transform the entire Pd/W(111) surface to a morphology composed completely of pyramidal {112} facets, the {011} faceting of Pd/W(111) occurs in coexistence with {112} faceting upon prolonged annealing. While {112} facets are found to grow in size (ranging from ~3 to 15 nm) with increasing annealing temperatures, the dimensions of {011} facets appear to be limited to ~2.5 nm. The coexistence of two types of pyramidal facets is consistent with energetic considerations based on first-principles calculations. The difference in their typical sizes is, on the other hand, interpreted as an evidence for kinetic factors in the faceting processes.
[S0163-1829(99)04315-5]

I. INTRODUCTION

The faceting of bcc(111) metal surfaces covered with certain adsorbed gases has been known for years,[1–3] and more recent evidence has been found for faceting induced by ultrathin metal films.[4–6] Unlike the atomically smooth, closely packed, low-index substrates that comprise the majority of published studies on model thin film metal-on-metal systems,[7–12] bcc(111) substrates represent atomically rough, morphologically unstable surfaces.

Studies in our laboratory have demonstrated that surfaces such as W(111) and Mo(111) coated with a single physical monolayer (ML) of certain metals (Pd, Rh, Ir, Pt, Au) undergo massive reconstruction from a planar morphology to a microscopically faceted surface upon heating to $T > 700$ K.[13] Others had previously reported faceting of bcc(111) surfaces induced by O and Cl.[1–3,14] Faceting has also been observed for metal film-covered W field emission tips.[7,15,16] Other atomically rough surfaces that exhibit faceting induced by adsorbed layers include fcc(210) surfaces.[17–19] In most of the studies on bcc(111) surfaces, the faceted morphology is found to comprise three-sided pyramids having {112} facets, based on low-energy electron diffraction (LEED) measurements[20,21] and scanning tunneling microscope (STM) work.[4,13,22,23] In the case of the Pt/W(111) system, STM studies also demonstrated a temperature dependence of facet sizes, ranging from ~3 to 100 nm, for increasing annealing temperatures.[23] In recent STM measurements, atomic resolution has been reported on faceted Pd/W(111) surfaces, confirming the {112} structures of individual facets.[13,22] While a critical coverage (~1 ML) has been identified as necessary to induce faceting on these surfaces,[20] a LEIS (low-energy ion scattering) study of the Pd/W(111) system shows further that a Pd monolayer remains on the outermost surface layer during the faceting transformation.[24] This implies that the overlayer metal film acts as a ''surfactant'' that induces faceting, and that there is substantial rearrangement of substrate atoms in the faceting process. When the initial coverage exceeds 1 ML, extra overlayer material forms three-dimensional clusters on top of the faceted structure, as identified by Auger electron spectroscopy[20] (AES) and STM.[22]

The faceting transition in these systems is believed to be thermodynamically driven but kinetically limited:[13,20] film-covered surfaces increase the anisotropy in surface free energy and enhance the relative stability of the faceted morphology.[25,26] A structural transition can occur when thermal annealing causes sufficient mobility of substrate and overlayer atoms. Recent theoretical studies of Mo(111) using first-principles methods[26] have shown that the calculated changes in surface free energy are consistent with the observed {112} faceting induced by various metal overlayers.

An intriguing aspect of the experimental results is that the dominant facet orientation is {112} rather than the close packed {011}, which is expected to be the most energetically stable surface in bcc metals. This fact is attributed primarily to the different changes in total surface area that occur for the formation of facets with different orientations. There is only an ~6% increase of the total surface area during {112} faceting on a bcc(111) surface in contrast to ~22% for {011} faceting. Consequently, {112} faceting may be more favorable energetically as a result of a greater reduction of the total surface energy. We will see from our first-principles calculations that this is indeed the case. Nevertheless, the formation of {011} facets on the Pd/W(111) can occur under certain conditions.

In this paper, we report conditions under which both {011} facets and {112} facets form and coexist on Pd/W(111) sur-

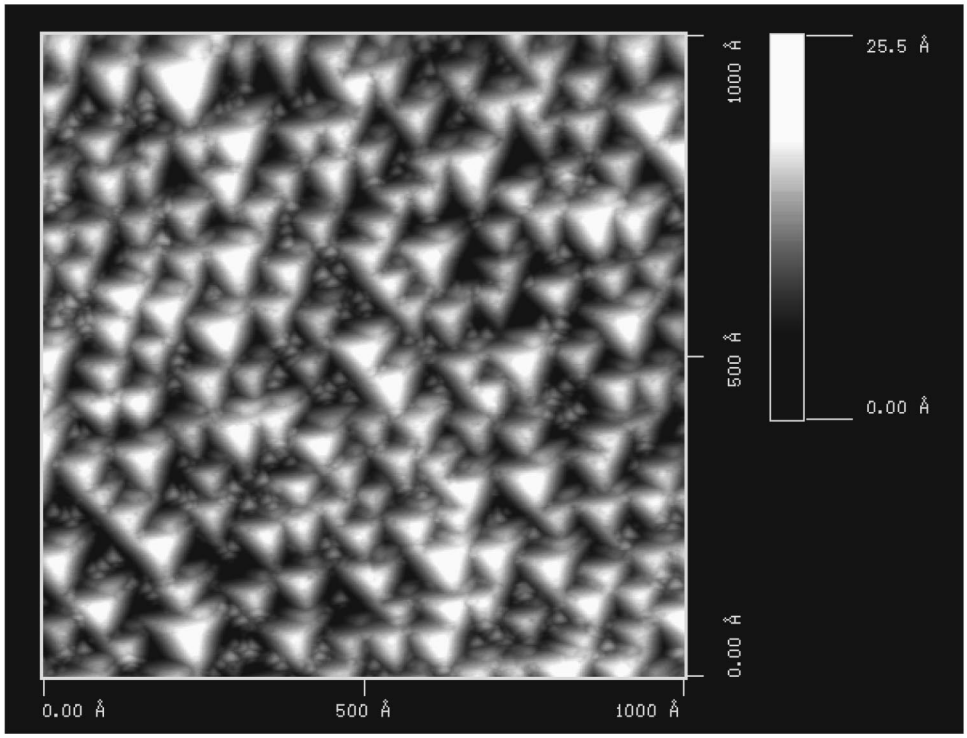

FIG. 1. Top view of a STM image showing the coexistence of {011} facets with {112} facets on a Pd/W(111) surface. The as-deposited coverage of Pd is 1.5 ML. Two types of three-sided pyramids form upon annealing at 1075 K for 9 min. The dimensions of this image are 100×100 nm and the vertical scale is 2.55 nm. The sample bias = +1 V.

faces. An interpretation of these observations based on first-principles calculations is also provided.

II. EXPERIMENTAL PROCEDURES

The detailed experimental setup used in these studies has been described elsewhere.[22] In brief, an ultrahigh vacuum (UHV) chamber with base pressures $<2\times10^{-10}$ torr is used. Among the measurement techniques available to us are AES, LEED, and a McAllister UHV STM.

A single-crystal tungsten rod with diameter ~8 mm is cut to obtain the disk-shaped sample, which is aligned by x-ray diffraction to within 0.5° of (111). Mechanical and chemical polishing are then employed to generate a mirror finish on the surface. This sample is then spot welded to one end of a hollow Mo cylinder which can be moved by an *X-Y-Z* rotary manipulator to permit LEED, AES, and STM measurements. In preparation for a typical STM measurement, the W surface is first cleaned by electron bombardment heating in UHV at a temperature above 2200 K. This is followed by heating in O_2 at about 1×10^{-7} torr to remove surface carbon segregating from the bulk. These steps are repeated until AES signals show less than 0.01 ML of C or O on the surface. We also verify long-range surface order by observing a sharp (1×1) LEED pattern from the clean surface.

Several segments of Pd wires spotwelded onto a tantalum sheet, which is then spotwelded to a W wire loop, serve as the Pd evaporation source. The resistively heated source is thoroughly outgassed before use, and the evaporator is surrounded with a liquid nitrogen cooled shield; pressures in the low 10^{-10} torr range are maintained during deposition. The deposition of a Pd overlayer is performed at a rate of 0.1 ML/min to the desired thickness. The relative overlayer coverage is determined by comparing the AES Pd/W peak ratio with precalibrated values based on temperature programmed desorption (TPD) and AES thermal stability measurements.[20] A critical Pd coverage $\theta_c\geqslant1$ physical monolayer [1.73×10^{15} atoms/cm^2 for W(111)] is required to initiate faceting.[20]

To initiate surface reconstruction of Pd-covered W(111), the sample is annealed to the desired temperature by electron bombardment heating from the rear of the sample. Prior to LEED and AES measurements, the sample is allowed to cool to ~300 K. The STM measurement is also performed at ~300 K with a typical sample bias (relative to the tip) of +0.2 to 1 V and a tunneling current of 1 nA.

III. RESULTS

Using LEED to identify {112} facets of Pd/W(111), Song, Dong, and Madey[20] found that the annealed surface becomes completely faceted, without identifiable regions of the planar (111) surface. Previous STM studies with atomic resolution[13,22] also confirm the formation of {112} facets, without coexisting planar (111) regions. In all of these studies, the faceting is induced by a Pd overlayer (>1 ML) upon annealing to 700 K or higher for 3 min.

We have found using STM that prolonged annealing of Pd/W(111) can cause the formation of pyramidal {011} facets that exist together with pyramidal {112} facets on Pd/W(111) surfaces. Figure 1 shows a STM image to illustrate this coexistence phenomenon. Following 9 min of thermal annealing at 1075 K, the W(111) surface covered by ~1.5 ML of Pd is observed to form microfacets. It is appar-

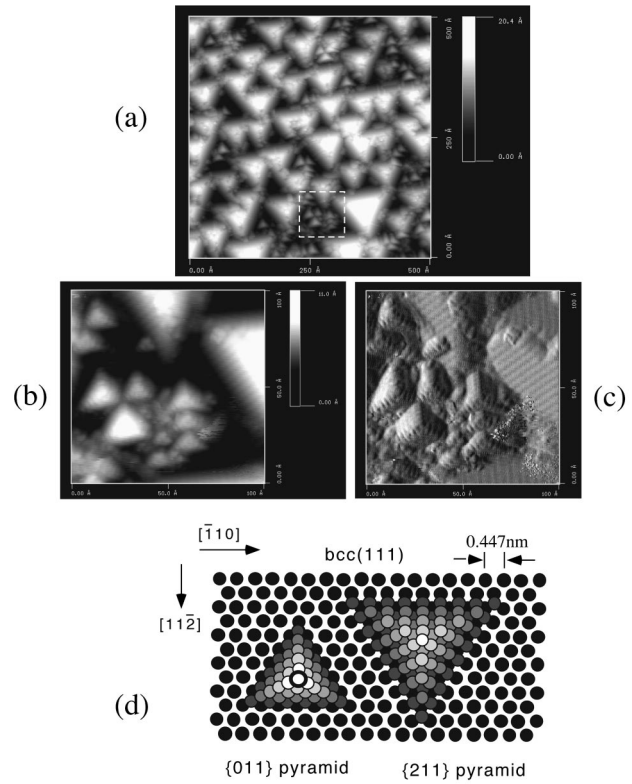

FIG. 2. (a) Top view of a STM image showing the coexistence of {011} facets with {112} facets on a Pd/W(111) surface. The as-deposited coverage of Pd is 1.0 ML. Two types of three-sided pyramids form upon annealing for 6 min. The dimensions of this image are 50×50 nm and the vertical scale is 2.0 nm. The sample bias $=+1$ V. The inset indicates the area shown in (b) with another scan. (b) Top view of a STM image showing the blown-up area in (a). The dimensions of this image are 10×10 nm and the vertical scale is 1.1 nm. The sample bias is equal to -0.5 V. (c) The differentiated image along the *x* direction (i.e., *x*-slope filtered image) of (b), revealing the atomic structures of each types of pyramidal facets. While the atomic rows on large facets identify themself as {112}, the atomic structures on tiny facets are quantitatively consistent with {011}. (d) Top view of a hard-sphere model showing the atomic structures of a pyramid with {011} facets and a pyramid with {112} facets on a bcc(111) surface. The indicated value of the atomic spacing corresponds to a bulk truncation structure of W(111), containing a pseudomorphic Pd overlayer.

ent that there are two different types of facets, each of which consists of three-sided pyramids with opposite orientations. While the major features are large three-sided pyramids with the apexes of their triangular bases pointing down, there are also tiny ones with apexes pointing up. (Note that Pd in excess of the ~1 ML coverage needed to induce faceting is found to agglomerate into three-dimensional clusters outside the field of view of this image, as in Ref. 22.)

A series of STM images with various scanned dimensions is shown in Fig. 2 for another Pd/W(111) surface where faceting of {011} and {112} are concurrent. While the as-deposited Pd coverage is only ~1.0 ML, a similar coexisting morphology again results from a prolonged annealing (6 min in this case). A blown-up image in the highlighted area of Fig. 2(a) is shown in Fig. 2(b), together with its differentiated version along the x direction (i.e., x-slope filtered image) displayed as Fig. 2(c), in which the atomic structures of each type of pyramidal facet can be identified. The facets that comprise the sides of the large pyramids have the familiar row-and-trough structure characteristic of a pseudomorphic Pd monolayer on W{112}, as discussed previously.[13,22]

The tiny pyramids in Fig. 2(c) are, on the other hand, identified as having {011} facets of W pseudomorphically coated by a Pd monolayer, for various reasons. First, the atomic arrangement of these facets [manifested in Fig. 2(c)] is consistent with the atomic structure of bcc{011} facets shown in the hard-sphere model of Fig. 2(d). Moreover, the numerical value of the observed atomic spacing is consistent (within the uncertainty of $\pm10\%$ associated with instrument calibration) with that in a bulk truncation model of a W substrate. In addition, the slopes of the sides of the faceted pyramids, measured with respect to the W(111) surface, are found to match the corresponding values for a bcc crystal within the instrumental uncertainty (The ratio of slopes is 2.0 ± 0.2, consistent with tilt angles of $\sim35°$ for {011} facets and $\sim19.5°$ for {112} facets). Thus, all of these comparisons are consistent with the formation of {011} facets covered by a pseudomorphic Pd monolayer, which coexist with Pd-covered {112} facets.

IV. CALCULATIONS

The total surface energy of the bcc(111) surface is given by $\gamma_{111}S$, where γ_{111} is the surface energy per unit area of the [111] orientation and S is total surface area. If the (111) surface facets to another orientation $\mathbf{b}=[hkl]$, and if edge energies are neglected, the surface energy after faceting is $\gamma_{\mathbf{b}}(S/\cos\theta)$, where $\gamma_{\mathbf{b}}$ is the surface energy per unit area of the new orientation $\mathbf{b}$, and θ is the angle between $\mathbf{b}$ and [111]. The change in surface energy is given by

$$\Delta E=\left(\frac{\gamma_{\mathbf{b}}}{\cos\theta}-\gamma_{111}\right)S. \tag{1}$$

This equation is correct for both $\mathbf{b}=[011]$ or [112] and is applicable as long as equivalent facets of the new orientation can maintain an average [111] orientation. The faceting transformation is energetically favorable if ΔE is negative.[27] If we express Eq. (1) in terms of the surface energy per surface unit cell, we have

$$\Delta E=\left(\sigma_{\mathbf{b}}\frac{A_{111}}{A_{\mathbf{b}}\cos\theta}-\sigma_{111}\right)N, \tag{2}$$

where N is the total number of surface sites on the topmost layer of the (111) surface [one geometric monolayer, 5.7×10^{14} atoms/cm^2 for W(111)], and $\sigma_{\mathbf{b}}$ and $A_{\mathbf{b}}$ are the surface energy per surface unit cell and the area of the primitive surface unit cell of orientation $\mathbf{b}$, respectively. For a bcc surface, we have

$$\frac{A_{\mathbf{a}}}{A_{\mathbf{b}}\cos\theta}=\frac{\delta_{\mathbf{a}}}{\delta_{\mathbf{b}}}\frac{\mathbf{a}\cdot\mathbf{a}}{\mathbf{a}\cdot\mathbf{b}}. \tag{3}$$

This purely geometrical relationship is good for two arbitrary orientations $\mathbf{a}$ and $\mathbf{b}$ in a bcc solid, and the factor δ_{hkl} equals 1 or 2 depending on whether $h+k+l$ is even or odd.

The change in surface energy when a surface of orientation **a** facets to equivalent facets of orientations **b** can thus be written as

$$\Delta E = \left(\sigma_{\mathbf{b}} \frac{\delta_{\mathbf{a}}}{\delta_{\mathbf{b}}} \frac{\mathbf{a}\cdot\mathbf{a}}{\mathbf{a}\cdot\mathbf{b}} - \sigma_{\mathbf{a}} \right) N. \quad (4)$$

For the special case of the $(111)\rightarrow\{011\}$ transformation, we take $\mathbf{a}=[111]$ and $\mathbf{b}=[011]$ and Eq. (4) reduces to

$$\Delta E_{(111)\rightarrow\{011\}} = (3\sigma_{011} - \sigma_{111})N, \quad (5)$$

while the change in surface energy in the $(111)\rightarrow\{112\}$ transformation is given by

$$\Delta E_{(111)\rightarrow\{112\}} = (\tfrac{3}{2}\sigma_{112} - \sigma_{111})N. \quad (6)$$

These equations are formally applicable to both the clean W surface and also to the W surface covered by wetting layers of Pd. In the latter case, the surface formation energies of Pd-coated W surfaces should be understood as

$$\sigma(\mathrm{Pd/W}) = \sigma(\mathrm{W}) + H(\mathrm{Pd/W}), \quad (7)$$

where $\sigma(\mathrm{W})$ is the orientation-dependent surface energy of the clean W surface, and H is the heat of formation of adsorbing a specific number of Pd overlayers on the W substrate. The heat of formation H depends on the Pd coverage as well as the substrate orientation, and is referenced to the bulk cohesive energy (we take H to be negative when the adsorption is exothermic).

If we examine a hard-sphere model of bcc surfaces, we will see that it takes one geometric monolayer to shadow the most compact bcc(011) surface, two geometric monolayers to shadow the (112) surface, and three geometric monolayers to shadow the most open (111) surface. These numbers, together with the correction for the angle between (011) or (112) facets and the planar (111), are the physical origin for the weighting factors 3 and 3/2 that appear in Eq. (5) and Eq. (6), respectively. It is more convenient if we describe the coverage of the Pd overlayers in terms of ''physical monolayers.'' A physical monolayer is defined as the number of geometric monolayers needed to shadow the substrate atoms in a particular surface orientation, and carries one, two, and three geometric monolayers for the (011), (112), and (111) surfaces, respectively. We can deduce from Eq. (3) that one physical monolayer of Pd covering a W(111) substrate carries exactly the same number of atoms as a physical monolayer covering a *faceted* (011) or a *faceted* (112) surface. In other words, when a W(111) surface covered by one physical monolayer of Pd transforms to triangular pyramids of {112} facets, no extra Pd atoms are required to cover the W(112) facets and no substrate W surface will be exposed. The same is true for the $(111)\rightarrow\{011\}$ transformation. As a consequence of this interesting geometric fact, the thermodynamic conditions [Eq. (5) and Eq. (6)] for faceting are independent of the absolute chemical potential of the Pd atoms.

The surface formation energies (σ) and the heats of formation (H) of Pd on W were calculated within the framework of the local density functional formalism[28] and norm-conserving pseudopotentials.[29] We used the standard slab geometry with a vacuum of approximately 10 Å . The repeated slabs have 11 layers of bcc W and additional pseudo-

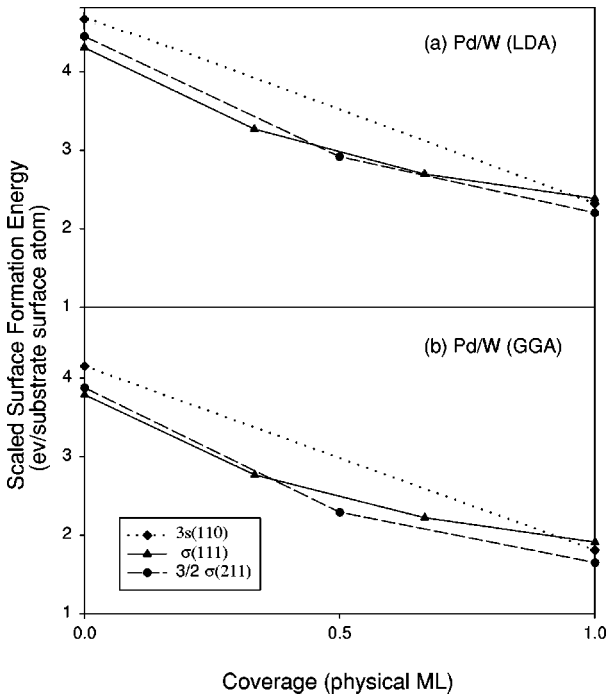

FIG. 3. Scaled surface formation energies per surface unit cell for Pd on W(111) (triangles), W(011) (squares) and W(112) (circles) as a function of Pd coverage, expressed as the number of physical monolayers. The surface formation energies for $\sigma_{(011)}$ and $\sigma_{(112)}$ have been weighted by geometrical factors of 3 and 3/2, respectively for direct comparison of the energy change during the faceting transformations. The lines serve as guides to the eyes. The results in the upper panel are calculated with LDA, and those in the lower panel are calculated with GGA.

morphoric overlayers of Pd are put on either side of the slabs. We employed plane waves with kinetic energy up to a cutoff of 11.5 Ry, augmented by Bloch sums of numerical orbitals centered at the atomic sites.[30] This mixed-basis approach has been applied successfully to study many transition metal surface problems,[31] and the overlayer-induced faceting of the Mo(111) surface.[26,32] The Hellmann-Feynman forces are calculated to relax all atomic degrees of freedom for each of the geometries under consideration. The convergence with respect to the screening potential and forces are accelerated by a recently proposed scheme.[33] For **k**-point sampling, we used an uniform $12\times12\times1$ grid in the surface Brillouin zones.

In Fig. 3, we compare σ_{111} with $\frac{3}{2}\sigma_{112}$ and $3\sigma_{011}$ for various Pd coverages. The Pd coverages are given in the number of physical monolayers covering the W substrate, and as we have noted already, a physical monolayer carries the same number of atoms on the flat (111) and faceted {011} and {112} surfaces. These surface formation energies per substrate atom, weighted by the proper geometric factors, can provide direct information about the faceting transformation according to Eq. (5) and Eq. (6).

At the clean surface limit (zero Pd coverage), we note from Fig. 3 that σ_{111} is lower than both $\frac{3}{2}\sigma_{112}$ and $3\sigma_{011}$. That means the clean W(111) surface is stable against faceting. The surface energies per unit area go in the order $\gamma_{011} < \gamma_{112} < \gamma_{111}$, but faceting is not energetically favorable be-

cause of the increase in total surface area in the faceting transformation [$\sim 6\%$ for $(111) \rightarrow \{112\}$ and $\sim 22\%$ for $(111) \rightarrow \{011\}$].

When Pd is adsorbed on the surface, we observe from Fig. 3 that the surface formation energies decrease for all three orientations. Since we used the energy of bulk Pd as reference in the calculation of the heat of formation, a decrease in σ as defined in Eq. (7) implies that Pd wets W(111), as well as W(112) and W(011). W has the highest surface energy among all metallic elements. It is energetically favorable for Pd, which has much lower surface energy, to wet W and cover exposed W surface atoms. In fact, our calculations[34] show that many fcc metals wet the W surface, although most of them do not dissolve in bulk W. We have calculated the surface formation energies at higher Pd coverages, and found that the surface formation energies are lowest for all three orientations at the physical monolayer coverage, beyond which the energy increases. This implies that at higher Pd coverage, it is more energetically favorable for excess Pd to form three-dimensional islands than to form overlayers. The growth mode of Pd on W is thus Stranski-Krastanov, with the W substrate covered by a wetting physical monolayer of Pd. This is true for (111), (011), and (112). These results have a simple geometrical interpretation: one physical monolayer corresponds to the number of atoms required to shadow all substrate atoms for different orientations. When the substrate is already covered by one physical monolayer of Pd, any additional adatoms are completely shielded from the W substrate by other Pd atoms. It would then be more energetically favorable for these excess Pd atoms to agglomerate into 3D clusters than to form strained overlayers.

While Pd adsorption lowers the surface formation energy significantly for all three orientations, the reduction of the surface formation energy is more significant for the more compact surfaces. This is evident from Fig. 3 where the slope of $3\sigma_{011}$ is found to be steeper than the average slope of $\frac{3}{2}\sigma_{112}$, which in turn is steeper than σ_{111}. The consequence is that the surface energy anisotropy becomes stronger, and both $\frac{3}{2}\sigma_{112}$ and $3\sigma_{011}$ are catching up with σ_{111}. At the coverage of one physical monolayer, $\frac{3}{2}\sigma_{112}$ and $3\sigma_{011}$ become lower than σ_{111}. According to Eq. (5) and Eq. (6), the system can gain energy by faceting from (111) to either {011} or {112}. The W(111) substrate becomes unstable when it is covered by one physical monolayer of Pd, and the faceting transformation is thermodynamically favorable from (111) to both the {112} and to {011} orientations. We further note from Fig. 3 that the system gains more energy by faceting to {112} than to {011}. This is consistent with the experimental observation that the faceted surface is dominated by pyramids of {112}-orientated faces. In terms of the surface formation energy per unit area, the (011) orientation always has the lowest energy. This the true for both the clean and Pd-coated W surface. However, the system energy is lowered more by the $(111) \rightarrow \{112\}$ faceting transformation because the surface area penalty is smaller: the 35.26° angle between {011} facets and the (111) is steeper than the 19.47° angle between {112} facets and (111).

We have checked the local-density approximation (LDA) results [Fig. 3(a)] with the generalized gradient approximation[35] (GGA) in the exchange correlation energy [Fig. 3(b)]. The absolute values of the *scaled* surface energies per surface atom are decreased by about 0.5 eV relative to the LDA results. The ordering of the surface energies at all coverages remains the same as the LDA results and all the conclusions we have deduced from the LDA calculations remain unchanged. In particular, the clean W(111) is stable, and at the Pd coverage of one physical monolayer, both (011) and (112) become lower than (111), with (112) having the lowest energy. We note that the difference in the scaled surface formation energies between (111) and (011) at one physical monolayer coverage is larger in GGA than in LDA, with (011) being clearly lower. Since GGA is (supposedly) more reliable than LDA, we have confidence that our results are not an artifact of the local-density approximation.

We note that total-energy calculations tell us whether a particular faceting transformation is thermodynamically allowed or not. One might therefore be tempted to extract the critical Pd coverage for the observed coexistence from the calculated results shown in Fig. 3. However, these $T=0$ calculations cannot predict straightforwardly when the onset should occur. From Fig. 3, the scaled surface energies $\sigma_{(111)}$ and $\sigma_{(011)}$ cross at a coverage of about 0.9 physical monolayer. This does not mean that the onset of the $(111) \rightarrow \{011\}$ transformation starts at 0.9 physical monolayers. First, the surface energies are calculated only at discrete coverages. Even if the surface free energies can be calculated at finite temperatures continuously as a function of coverage and thereby produce smooth curves, the onset of the transformation should be given by a common tangent construction, rather than the crossing of the two scaled energy curves. This procedure certainly requires many more data points than have been shown in Fig. 3. More importantly, the onset and the limiting of such transformations should largely be governed by the kinetics rather than energetics.

From both Figs. 1 and 2, we note the relatively small size of {011} facets (typically 2.5nm) compared to that of the coexisting {112} facets (~ 8 to ~ 12 nm). We believe that the delayed onset of growth of {011} facets, as well as the differences in the limiting size of the {011} and {112} facets, are due to kinetic effects in the facet growth process. As discussed previously,[26] there is an activation barrier to the nucleation and growth of pyramidal facets, which depends on a competition between surface free energy, edge energy, and apex energy. The barrier is higher for larger edge and apex energies, while it is smaller for bigger surface energy difference as given by Eq. (1). These energies are expected to be different for {011} and {112} facets. Our calculation shows that the surface energy difference is smaller for the case of {011} than for {112}. In addition, the total edge energies should be bigger in the {011} pyramids since they have sharper edges and the ratio of the edge length to surface area is greater for {011} than for {112} pyramids. These effects indicate that the {011} pyramids should have a higher formation barrier. Moreover, if the facet makes an angle θ with the surface, the number of atoms in the pyramid bounded by the facets is proportional to $\tan\theta$. Thus, the number of atoms needed to form a {011} pyramid is about twice the number needed to form a {112} pyramid. Since the formation of pyramids mandates a massive transport of surface atoms, it is not surprising that the growth of {011} pyramids should proceed more slowly than the growth of {112} pyramids.

Based on a hypothetical process of facet growth, we can also suggest an alternative kinetic mechanism to explain the occurrence of {011} faceting upon prolonged annealing. Since the continuous growth of {112} facets upon annealing implies a sequential reduction of the total number of {112} pyramids per unit area [projected onto the (111) plane], it is reasonable to assume that some pyramids are depleted to ''feed'' neighboring, growing pyramids. By studying a hard-sphere model for the structural relationships between {011} and {112} pyramids, we realize that a highly probable mechanism for depletion of a small {112} pyramid is to remove atomic layers slice-by-slice along {011} planes. Furthermore, the removed atoms are likely to add other layer(s) mainly onto adjacent {112} facets of nearest-neighbor pyramids, due to the Ehrlich-Schwoebel potential that hinders diffusion over facet edges. When the typical size of {112} facets has grown larger upon prolonged annealing, the depletion of the {011} ''feeder'' pyramids will have less chance to be completed, leading to their stabilization. A more quantitative development of this model is underway and will be reported elsewhere.

V. SUMMARY

In short, triangular-based pyramids with {011} facets are observed to coexist with {112} pyramids in the Pd/W(111) system using STM. These observations are consistent with first principles calculations which show that it is energetically favorable for {111} to transform to either {112} or {011}.

ACKNOWLEDGMENTS

The Rutgers work was supported by the U.S. Department of Energy, Office of Basic Energy Sciences. T.C.L. was supported by (NSC)87-2112-M-194-008, and a grant of computer time at the National Center for High-Performance Computing. C.T.C. and J.G.C. were supported by RGC Hong Kong through HKUST694/96P. C.T.C. thanks AMRI-HKUST and SS-HKUST for providing CPU time.

*Authors to whom correspondence should be sent: madey@physics.rutgers.edu; phchan@ust.hk

†Present and permanent address: Department of Physics, Fudan University, Shanghai, China.

[1] N. J. Taylor, Surf. Sci. **2**, 544 (1964).

[2] J. C. Tracy and J. M. Blakely, Surf. Sci. **13**, 313 (1968).

[3] C. Zhang, M. A. van Hove, and G. A. Somorjai, Surf. Sci. **149**, 326 (1985).

[4] T. E. Madey, J. Guan, C.-Z. Dong, and S. M. Shivaprasad, Surf. Sci. **287/288**, 826 (1993).

[5] T. E. Madey, K.-J. Song, C.-Z. Dong, and R. A. Demmin, Surf. Sci. **247**, 175 (1991).

[6] K.-J. Song, R. A. Demmin, C.-Z. Dong, E. Garfunkel, and T. E. Madey, Surf. Sci. **227**, L79 (1990).

[7] E. Bauer, in *The Chemical Physics of Solid Surfaces and Heterogeneous Catalysis*, edited by D. A. King and D. P. Woodruff (Elsevier, Amsterdam, 1984), p. 1.

[8] J. A. Rodriguez, S. Y. Li, J. Hrbek, H. H. Huang, and G.-Q. Xu, J. Phys. Chem. **100**, 14 476 (1996).

[9] C. T. Campbell, Annu. Rev. Phys. Chem. **41**, 775 (1990).

[10] S. Chang and P. A. Thiel, Crit. Rev. Surf. Chem. **3**, 239 (1994).

[11] S. M. Davis and G. A. Somorjai, in *The Chemical Physics of Solid Surfaces and Heterogeneous Catalysis*, edited by D. A. King and D. P. Woodruff (Elsevier, Amsterdam, 1982), p. 217.

[12] J. A. Rodriguez and D. W. Goodman, Surf. Sci. Rep. **14**, 1 (1991).

[13] T. E. Madey, J. Guan, C.-H. Nien, C.-Z. Dong, H.-S. Tao, and R. A. Campbell, Surf. Rev. Lett. **3**, 1315 (1996).

[14] F. Bonczek, T. Engel, and E. Bauer, Surf. Sci. **97**, 595 (1980).

[15] A. Cetronio and J. P. Jones, Surf. Sci. **40**, 227 (1973).

[16] K. Pelhos, T. E. Madey, and R. Blasczyszyn, Surf. Sci. (to be published).

[17] M. Sander, R. Imbihl, R. Schuster, J. V. Barth, and G. Ertl, Surf. Sci. **271**, 159 (1992).

[18] R. E. Kirby, C. S. McKee, and L. V. Renny, Surf. Sci. **97**, 457 (1980).

[19] R. E. Kirby, C. S. McKee, and M. W. Roberts, Surf. Sci. **55**, 725 (1976).

[20] K.-J. Song, C.-Z. Dong, and T. E. Madey, Langmuir **7**, 3019 (1991).

[21] J. Guan, R. A. Campbell, and T. E. Madey, Surf. Sci. **341**, 311 (1995).

[22] C.-H. Nien and T. E. Madey, Surf. Sci. **380**, L527 (1997).

[23] C.-Z. Dong, S. M. Shivaprasad, K.-J. Song, and T. E. Madey, J. Chem. Phys. **99**, 9172 (1993).

[24] C.-Z. Dong, L. Zhang, U. Diebold, and T. E. Madey, Surf. Sci. **322**, 221 (1995).

[25] S. P. Chen, Surf. Sci. **274**, L619 (1992).

[26] J. G. Che, C. T. Chan, C. H. Kuo, and T. C. Leung, Phys. Rev. Lett. **79**, 4230 (1997).

[27] C. Herring, Phys. Rev. **82**, 87 (1951).

[28] See, e.g., *Theory of the Inhomogeneous Electron Gas*, edited by N.H. March and S. Lundqvist (Plenum, New York, 1983), and references therein; L. Hedin and B. I. Lundqvist, J. Phys. C **4**, 2064 (1971).

[29] See, e.g., G. B. Bachelet and M. Schlüter, Phys. Rev. B **25**, 2103 (1982).

[30] S. G. Louie, K. M. Ho, and M. L. Cohen, Phys. Rev. B **19**, 1774 (1979); C. Elsasser, N. Takeuchi, K. M. Ho, C. T. Chan, P. Braun, and M. Fahnle, J. Phys.: Condens. Matter **2**, 4371 (1990); K. M. Ho, C. Elsässer, C. T. Chan, and M. Fähnle, *ibid.* **4**, 5189 (1992).

[31] See, e.g., C. T. Chan, K. M. Ho, and K. P. Bohnen, in *Handbook of Surface Science*, Vol. I, edited by W. N. Unertl (Elsevier, Amsterdam, 1996), Chap. 3.

[32] J. G. Che and C. T. Chan, Surf. Sci. **401**, L432 (1998).

[33] C. T. Chan, K. P. Bohnen, and K. M. Ho, Phys. Rev. B **47**, 4771 (1993).

[34] T. C. Leung and C. T. Chan (unpublished).

[35] J. P. Perdew, K. Burke, and M. Ernzerhof, Phys. Rev. Lett. **77**, 3865 (1996).